We are IntechOpen, the world's leading publisher of Open Access books Built by scientists, for scientists

4,800
Open access books available

122,000
International authors and editors

135M
Downloads

Our authors are among the

154
Countries delivered to

TOP 1%
most cited scientists

12.2%
Contributors from top 500 universities

CLARIVATE ANALYTICS BOOK CITATION INDEX INDEXED

WEB OF SCIENCE™

Selection of our books indexed in the Book Citation Index in Web of Science™ Core Collection (BKCI)

Interested in publishing with us?
Contact book.department@intechopen.com

Numbers displayed above are based on latest data collected.
For more information visit www.intechopen.com

Chapter 5

Machining Characteristics of Direct Laser Deposited Tungsten Carbide

Paweł Twardowski and Szymon Wojciechowski

Additional information is available at the end of the chapter

http://dx.doi.org/10.5772/51439

1. Introduction

Machinability can be defined as the relative susceptibility of the work material to the decohesion phenomenon and chip formation, during cutting and grinding. This feature depends on work and tool's material physic-chemical properties and condition, method of machining, as well as cutting conditions [1]. Therefore, there is no unique and unambiguous meaning to the term machinability. This feature, can be described by many various indicators. Each one of them carries out a wide variety of operations, each with a different criteria of machinability. A material may have good machinability by one criterion, but poor machinability by another [2].

To deal with this complex situation, the approach adopted in this chapter is to divide machinability indicators into two groups, namely: physical and technological indicators. Physical machinability indicators include i.a. temperatures, cutting forces, vibrations and residual stresses generated during machining process, because their value have the direct influence on the ensemble of the remaining machining effects. Technological indicators include mainly machined surface texture and tool's life (relatively tool wear).

The most popular method for producing tungsten carbide components is by powder metallurgy technology. Nonetheless, for individual, small quantity production or product prototyping this method is too costly and time consuming. The alternative to powder metallurgy is Direct Laser Deposition (DLD) technology, which can be used to quickly produce metallic powder prototypes by a layer manufacturing method [3, 4] – Figure 1. The primary objective of DLD technology is the regeneration of machine parts or machine parts manufacturing with the improved surface layer properties, e.g. higher corrosion, erosion and abrasion resistance. Direct Laser Deposition is an extension of the laser cladding process, which enables three dimensional fully-dense prototype building by cladding consecutive layers on top of one another [6]. The DLD technology is increasingly being used

in production of functional prototypes, modify or repair components which have excellent hardness, toughness, corrosion and abrasion wear-resistance, e.g. machine parts for the automotive industry – Figure 2. In the near future DLD technology will be used in manufacturing of spare parts in long term space missions [7] or submarines [8].

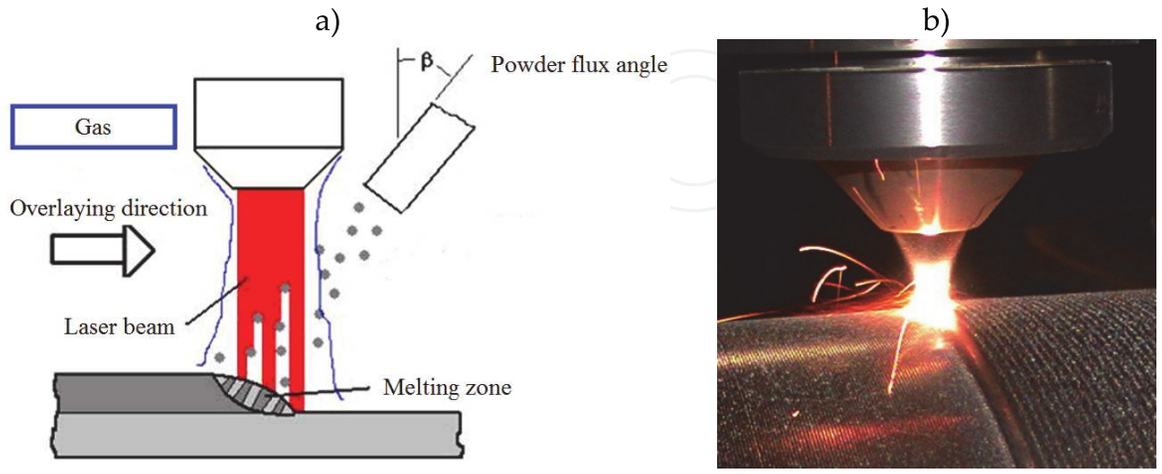

Figure 1. Direct laser deposition technology (DLD): a) the scheme of process, b) the view of process [5]

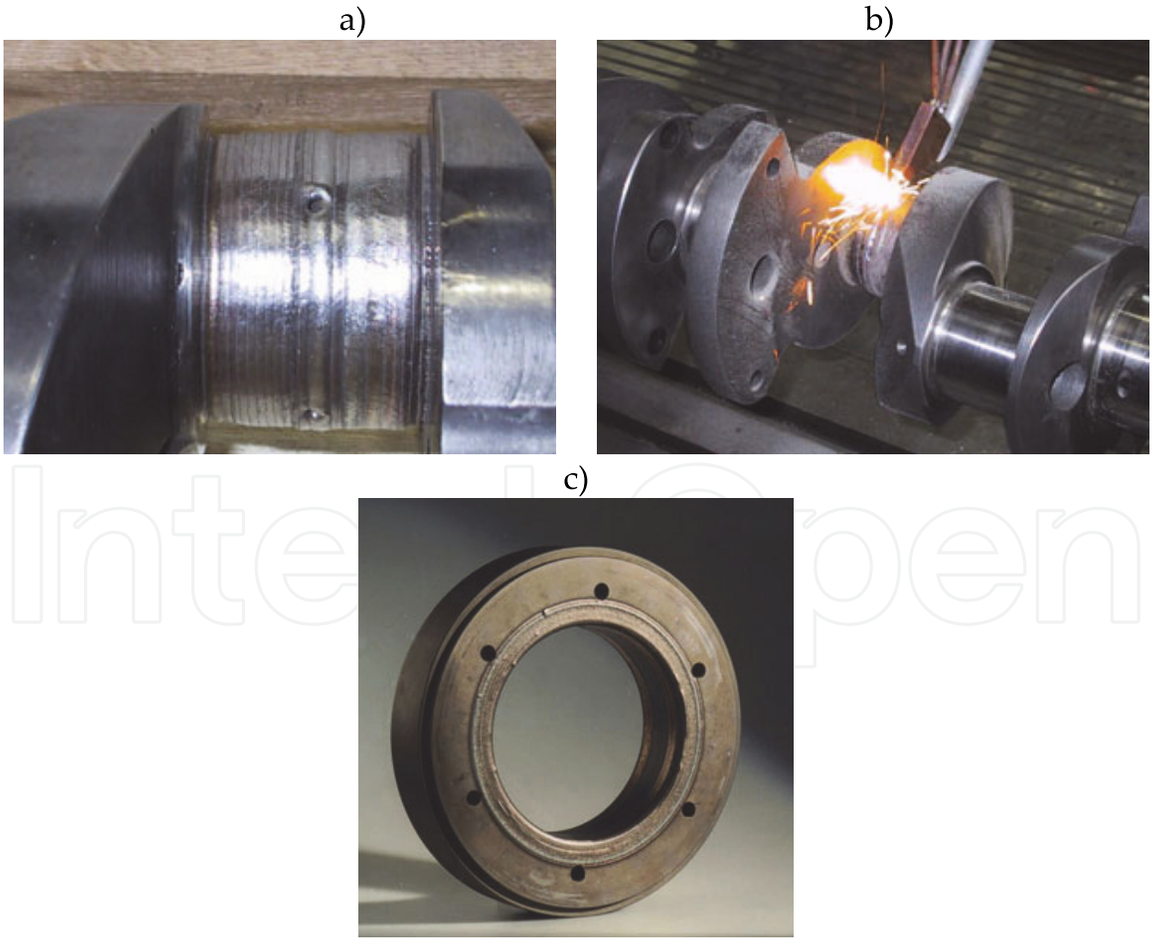

Figure 2. The application of DLD technology for the crankshafts (a, b) and parts for the automotive industry (c) [5]

Unfortunately, DLD technology has also significant disadvantage. Presently most components produced by DLD technology has an unsatisfactory geometric accuracy as well as surface roughness and requires some post-process machining to finish them to required tolerances [9]. Therefore, the machinability of DLD manufactured materials (e.g. tungsten carbide), require further and extensive studies.

2. Machining of tungsten carbide

Tungsten carbide has excellent physicochemical properties such as, superior strength, high hardness, high fracture toughness, and high abrasion wear-resistance. These properties impinges wide application of tungsten carbide in industry for cutting tools, molds and dies. On the other hand, these unique properties can cause substantial difficulties during machining process, which can result in low machinability. Therefore, machining of tungsten carbide requires the knowledge about the physical effects of the process, as well as appropriate selection of machining method and cutting conditions, enabling desired technological effects. The primary objective of post-process machining of tungsten carbide is to achieve satisfactory geometric and physical properties of its surface texture.

The most popular finishing method of tungsten carbides applied in the tooling industry is grinding with the diamond and CBN (cubic boron nitride) wheels. However, in order to produce optical components made of cemented carbide (e.g. spherical mirrors) the profile quality requires a low surface roughness, a stringent form accuracy on the submicron scale, as well as a low amount of surface damage [10]. Traditional grinding with the diamond wheels can cause machining-induced cracks and damages to the material. To remove these cracks and damage and to obtain a mirror finish, lapping and polishing with fine diamond abrasives are usually employed. Nevertheless, these processes can cause the deterioration of form accuracy and increase the machining cost.

Recently, ultraprecision grinding has been developed that substantially decreases subsurface damage and can precisely control the geometry of the finished surface [11, 12]. This kind of process is conducted on the ultraprecision CNC grinding machines, with three-axes movements, and micro-system to deterministically generate, fine, and pre-polish a plano or spherical surface. Very often these machines have motors with power exceeding 1kW and maximal rotational speeds above 80 000 rpm. The example of ultraprecision set-up is shown in Figure 3a.

Tools applied in the ultraprecision grinding processes are usually selected as metal-bond diamond cup wheels (Figure 3b) with grit sizes between 15÷25 μm. The selected CNC grinding program includes two parts, i.e. stock removal and spark out. During the stock removal step, the grinding speed is selected in the range of 10÷15 m/s (for a small tool diameters it corresponds to rotational speeds up to 40 000 rpm). The vertical feed rates of the tool spindle are usually selected in the range of 0.05÷0.2 mm/min, and the workpiece spindle rotated at 1000 rpm. During the spark out phase, the workpiece is rotated with a 1000 rpm for about 180 rotations.

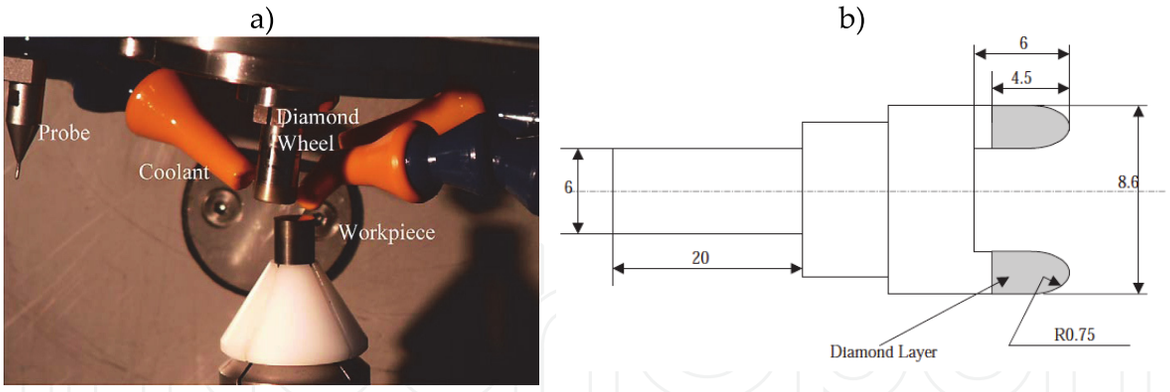

Figure 3. The ultraprecision grinding process of a spherical mirrors: a) set-up [10], b) schematic presentation of the diamond tool [12]

Apart of grinding, recently are seen tendencies to cutting (mainly turning and milling – Figure 4) brittle materials such as, tungsten carbide and reaction-bonded silicon carbide (RB-SiC) by a superhard CBN (cubic boron nitride) and PCD (polycrystalline diamond) cutters in cutting conditions assuring ductile cutting [13, 14]. This technique of cutting can be achieved when depths of cut and feeds (expressed as uncut chip thickness) are extremely low and a quotient of the tool cutting edge inclination angle to uncut chip thickness is greater than unity ($r_n/h>1$). In milling process of tungsten carbide by CBN tools, the transition from ductile to brittle cutting occurs at critical depth of cut $a_{pcr.}$ equal to approximately 4.78 μm. Machining with very low cutting conditions is feasible only on ultraprecision machine tools with high rigidity, which is substantial limitation of this technique.

Figure 4a depicts the schematic diagram of the numerically controlled three-axis ultraprecision lathe used in ductile turning experiments. The lathe has two perpendicular hydrostatic tables along the X- and Z-axis direction, in addition to a B-axis rotary table built into the X-axis table. Both X-axis and Z-axis tables have linear resolutions of 1nm, and the B-axis rotary table has an angular resolution of one ten millionths of a degree. The sample can be rotated with the spindle and moved along the Z-axis direction, while the cutting tool can be moved along the X-axis direction and also rotated around the B-axis.

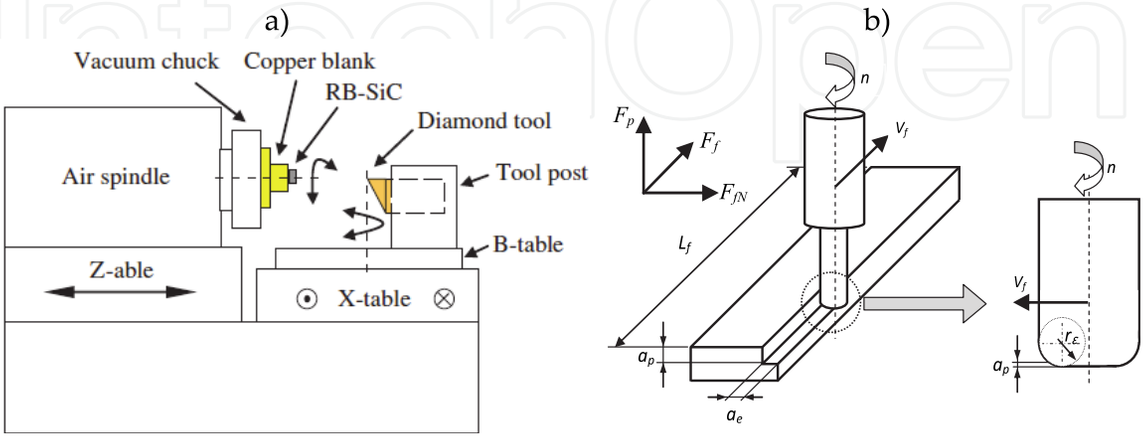

Figure 4. The set-up of cutting process: a) ductile turning of carbides [15], b) face milling of DLD tungsten carbide [16]

Cutters applied in the ductile cutting experiments, are made of diamond (MCD, PCD) or CBN (cubic boron nitride) materials. The example of turning and milling tool applied in carbide's machining process is presented in Figure 5. These tools have usually negative geometry (rake γ angles lower than 0), and a small values of tool cutting edge inclination angle r_n < 6 μm, which is needed to initiation of the ductile cutting. To obtain a crack free surface the tool feed rate f and the cutting depth a_p must be very low. Their values are usually selected as: $f \approx 1 \div 75$ μm/rev and $a_p \approx 2 \div 10$ μm. Cutting speeds can be selected in the following range: $v_c = 50 \div 600$ m/min.

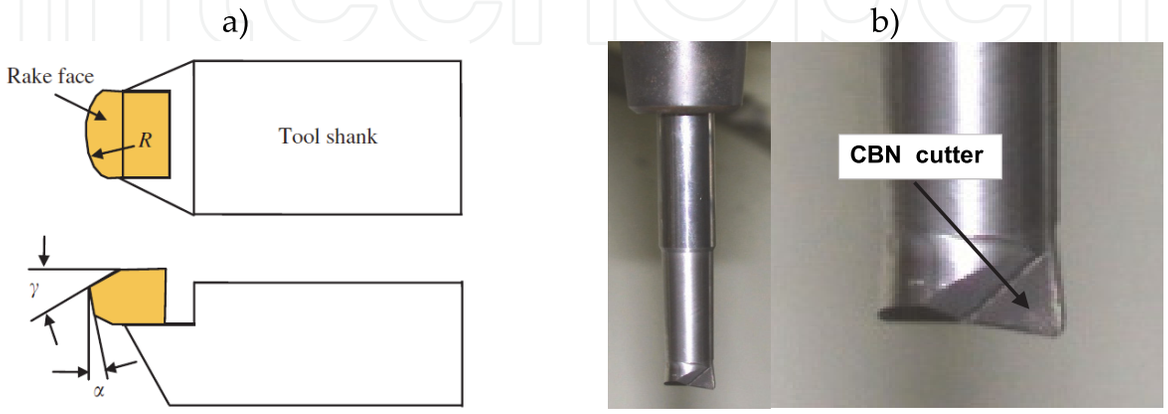

Figure 5. Tools applied in machining of carbides: a) diamond turning tool [15], b) CBN torus end mill [16]

In order to finish plane surface, made of tungsten carbide, obtained using DLD technology, one can apply face milling process (Figure 4b). Surfaces obtained using DLD technology have significantly higher roughness than ones manufactured by powder metallurgy technology. Therefore, cutting parameters during machining of these surfaces can be higher than those applied in machining of powder metallurgy surfaces, and selected as follows: feed per tooth $f_z \approx 25 \div 100$ μm/tooth, axial depth of cut $a_p = 20$ μm, radial depth of cut $a_e = D/2$ (half of tool's diameter).

3. The analysis of physical machinability indicators

In this chapter the analysis of main physical machinability indicators, such as: cutting forces and vibrations will be presented. The set-up of cutting forces and vibrations measurements during face milling process is presented in Figure 6.

The hook up into bed of a machine piezoelectric force dynamometer was used to measure total cutting forces components [16]. Instantaneous force values were measured in feed force F_f, normal feed force F_{fN} and thrust force F_p directions. Force dynamometer's natural frequency is equal to 1672 Hz. In order to avoid disturbances induced by proximity of forcing frequency to gauge natural frequency, the band – elimination filter was applied. The acceleration of vibrations of tungsten carbide workpiece during milling was measured using piezoelectric accelerometer. These vibrations were measured in the same directions as cutting force components.

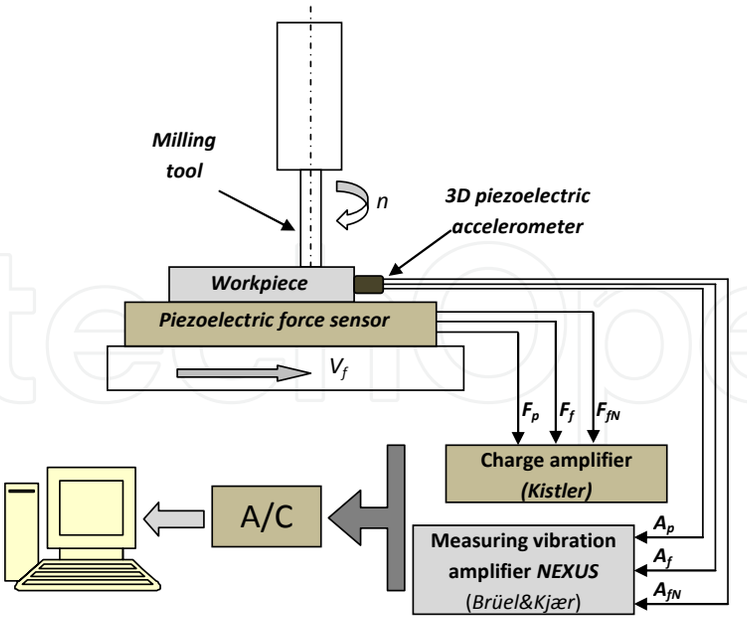

Figure 6. The set-up of force and vibration measurements during face milling of tungsten carbide [16]

Figure 7 depicts the tool wear (VB_c) influence on *RMS* values of vibrations A_p and forces F_p.

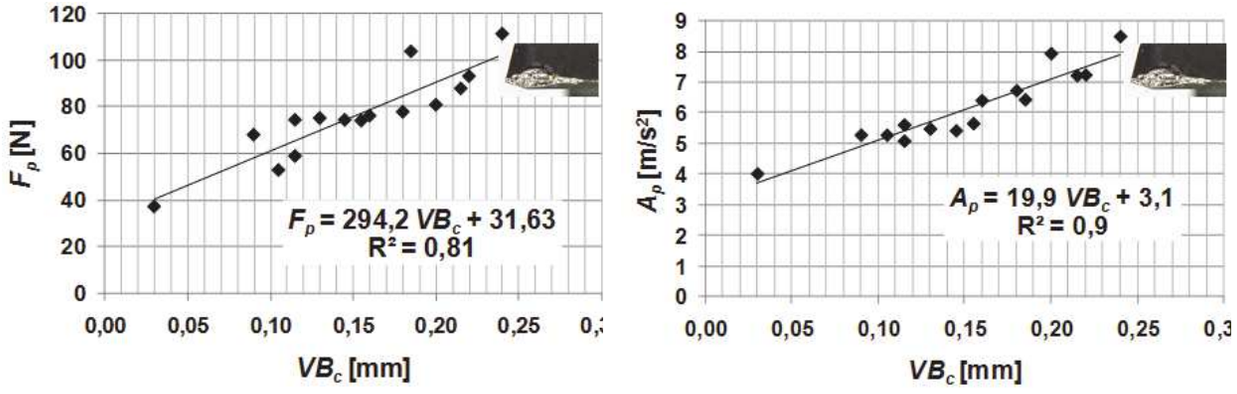

Figure 7. *RMS* values of thrust force F_p and thrust vibrations F_p in function of tool wear VB_c. Cutting conditions: v_c = 68 m/min, v_f = 180 mm/min, a_p = 0.02 mm, a_e = 6 mm

On the base of conducted investigations, clear relation between progressing tool wear and *RMS* values of forces and vibrations in thrust direction (F_p, A_p) can be seen. Above-mentioned relation is expressed by the correlation coefficient R^2>0.8. Tool wear growth induced force F_p and vibration A_p increase, which stays in agreement with investigations [17] related to machining of hardened steel. It was stated that in machining process of tungsten carbide typical abrasion wear, (characterized by VB_c indicator) concentrated mainly on flank face can be found. This phenomenon is probably caused by a friction of hard carbide particles on CBN tool flank face [18]. As a result, progressing abrasion of the tool binder induces the growth of friction force, which in turn is related to force and vibration (F_p, A_p) increase. It is necessary to mention that, in remaining cutting force and vibration directions (F_f, A_f, F_{fN}, A_{fN}) no correlation with tool wear VB_c was found out (correlation coefficient R^2 was lower than 0.1).

In order to analyze forcing frequencies affecting cutting force components during milling of tungsten carbide, the FFT (Fast Fourier Transform) spectra were determined (Figure 8). From the Figure 8 it is resulting, that primary forcing frequency is tooth passing frequency *zfo*. Since number of teeth: *z*=2, the *zfo* frequency overlaps with the second harmonics of spindle speed frequency – 2*fo*. Therefore 2*fo* and *zfo* frequencies are dominant. It means that the dominative factor in F_{fN} and F_p force time courses is milling process kinematics related to the cutting force generated by the each of teeth. Primary harmonic component *zfo* is accompanied by so-called „collateral bands" with the following values: *zfo* + *fo* and *zfo* – *fo*. They appearance is related to the occurrence of radial run out phenomenon. From the Figure 8 it can be also seen that frequency spectra of F_{fN} and F_p force components consist of spindle speed frequency polyharmonics. Similar dependencies were observed for majority of investigated cutting force components frequency spectra.

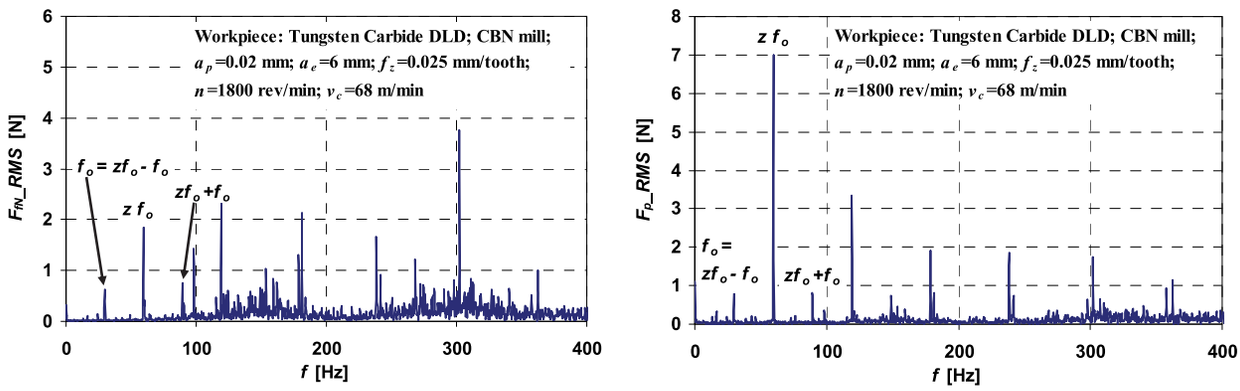

Figure 8. Frequency spectra of F_{fN} and F_p force components

Figure 9 compares cutting forces in function of feed per tooth obtained during milling of tungsten carbide and hardened X153CrMoV12 steel (with 60 HRC hardness). It was observed that both in milling of tungsten carbide and hardened steel, cutting forces (F_f, F_{fN}, F_p) are increasing monotonically with feed per tooth f_z growth, what is typical dependency occurring in metal cutting processes. In tungsten carbide milling process, the highest force values appeared in thrust direction (F_p), independently of feed per tooth f_z value. As it was mentioned before, this phenomenon is probably caused by a friction of hard carbide particles on CBN tool flank face, which affects tool wear increase, and hence friction and thrust force F_p growth (it is worth indicating that after second experimental trial tool wear was $VB_c \approx 0.07$ mm). In case of milling of hardened steel, thrust force F_p has lower values than those obtained during milling of tungsten carbide. This is attributed to the significantly lower hardness of hardened steel (in comparison to tungsten carbide), which reduces tool wear intensity (tool wear after second trial: $VB_c \approx 0$), and thus values of thrust force F_p. The influence of work material's hardness on the cutting force values during machining is described in details in [19].

Figure 10 depicts *RMS* values of vibrations in function of feed per tooth f_z during milling of tungsten carbide.

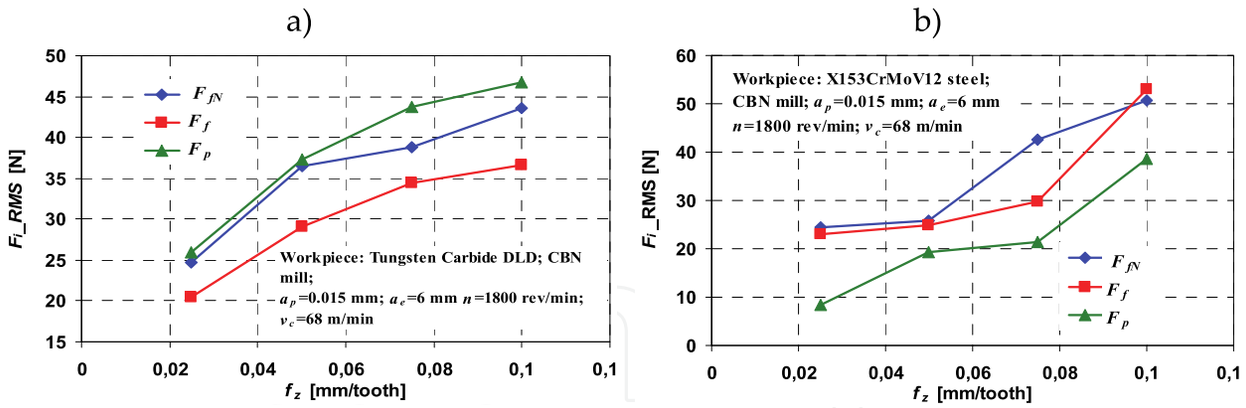

Figure 9. *RMS* values of force components in function of feed per tooth f_z in milling of: a) tungsten carbide, b) hardened steel

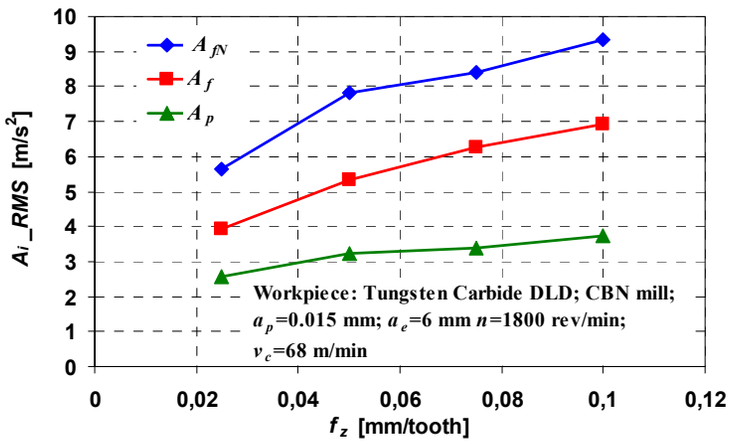

Figure 10. *RMS* values of vibrations (A_f, A_{fN}, A_p) in function of feed per tooth f_z in milling of tungsten carbide

From the Figure 10 it can be seen, that feed per tooth f_z growth induces monotonic increase of vibrations in all measured directions (A_f, A_{fN}, A_p). It was observed that independently of feed per tooth f_z value, vibrations in the thrust direction A_p have the smallest values, in comparison to the other measured directions. The reason of this phenomenon is probably connected with the highest tool stiffness in the thrust direction (parallel to rotational axle). The highest acceleration of vibration values (independently of feed per tooth f_z value) occurred in the feed normal direction A_{fN}. According to research: [20, 21], it could be caused by the direct contact of cutter radius and tool flank face with the machined surface, which is the major source of forcing vibrations, and also the smallest damping ratio in the feed normal direction compared to the other two axes.

In order to estimation of cutting forces in the broad range of cutting conditions, cutting force models can be applied. Majority of models assume that cutting force is proportional to sectional area of cut and the specific cutting pressures. Figure 11 depicts, empirically determined course of the specific cutting pressure in function of mean uncut chip thickness k_i=f(h), in milling of tungsten carbide, while table 1 specific cutting pressure (k_c, k_{cN}, k_p) regression equations.

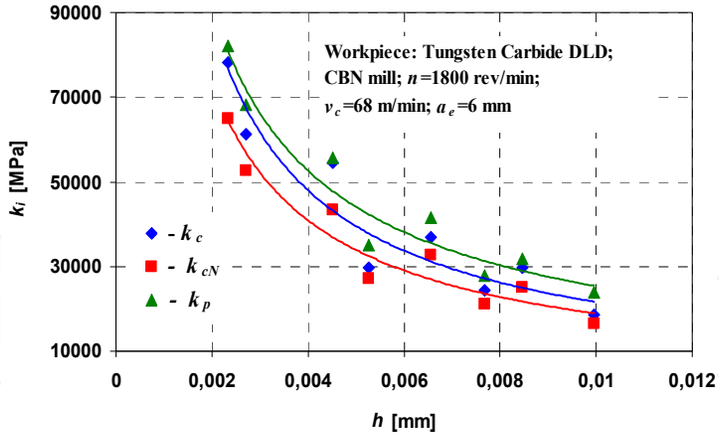

Figure 11. Specific cutting pressure k_i in function of mean uncut chip thickness h

From the Figure 11 it can be seen, that mean uncut chip thickness h growth is accompanied by the specific cutting pressure (k_c, k_{cN}, k_p) decrease. This phenomenon stays in agreement with the dependency observed in metal cutting processes. Between experimental specific cutting pressure values and calculated ones (based on regression analysis) some divergences can be seen. These divergences are expressed by the correlation coefficient R^2>0.87 (table 1). Above-mentioned divergences have disadvantageous influence on mechanistic cutting force model accuracy. The reason of their occurrence could be attributed to milling process dynamics (e.g. machine tool stiffness).

Specific cutting pressure component	Specific cutting pressure k_i	
	Regression equation	R^2
Tangential	$k_c = 388.9\ h^{-0.872}$	0.873
Radial	$k_{cN} = 385.4\ h^{-0.845}$	0.901
Thrust	$k_p = 644.1\ h^{-0.798}$	0.915

Table 1. Regression equations of specific cutting pressure components

4. The analysis of technological machinability indicators

Machined surface texture and tool wear are the essential factors determining cutting ability in practical applications. One of the most popular geometrical tool wear indicators is tool wear on the flank face designated by the VB. Its value can be measured using stereoscopic microscopes. The method of tool wear measurement is depicted in Figure 12. Machined surface texture can be examined using three and two dimensional (3D, 2D) measurements. 3D measurements can be achieved using stationary profilometer Hommelwerke T8000 (Figure 13). Two dimensional measurements can be made by T500 profilometer (Hommelwerke), equipped with T5E head and Turbo DATAWIN software. The sampling length lr = 0.8 mm, the evaluation length $ln = 5 \cdot lr$ = 4.8 mm, the length of wave cut – off λc (cut – off) = 0.8 mm and ISO 11562(M1) filter are usually applied in the measurements. As a result of 2D measurements the surface profile charts are received. On the basis of surface profile charts the Ra and Rz parameters can be calculated using appropriate software.

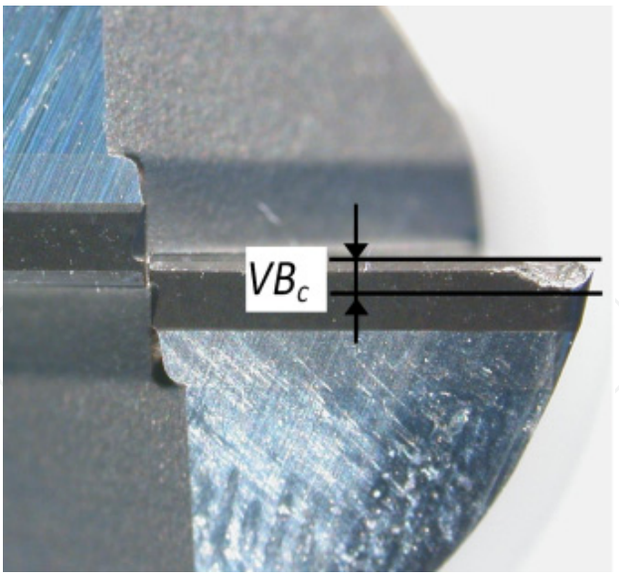

Figure 12. Tool's flank wear measurement

Figure 13. The view of stationary profilometer Hommelwerke T8000

Figure 14 depicts the tool wear progress in function of cutting time during face milling of tungsten carbide (manufactured by DLD technology) with CBN cutters. As it can be seen, tool wear process for each tooth is similar, i.e. there are no significant deviations of VB_c values for respective teeth. Introducing arbitrary dullness criterion VB_c = 0.2 mm, it can be seen that twofold cutting speed v_c increase, caused almost eightfold tool life T decrease. On the basis of acquired data the s exponent used in Taylor`s equation ($T = C_T/v_c^s$, where C_T is constant dependent of workpiece properties) can be estimated, but it is necessary to emphasize that determining the s exponent from two experimental values is not very accurate. After consideration of the v_{c1}, v_{c2}, T_1 and T_2 the s = 2.65 was obtained. This value is located in the range of the s exponents characteristic for high speed milling of hardened steel, thus the intensity of cutting speed v_c influence on tool life T in tungsten carbide milling is similar to those for hardened steel. Moreover the tool wear concentrates on the flank face of the tool (see Figure 14c). Because of this, the relations between the tool wear and both forces and vibrations in thrust direction were observed (see Figure 7).

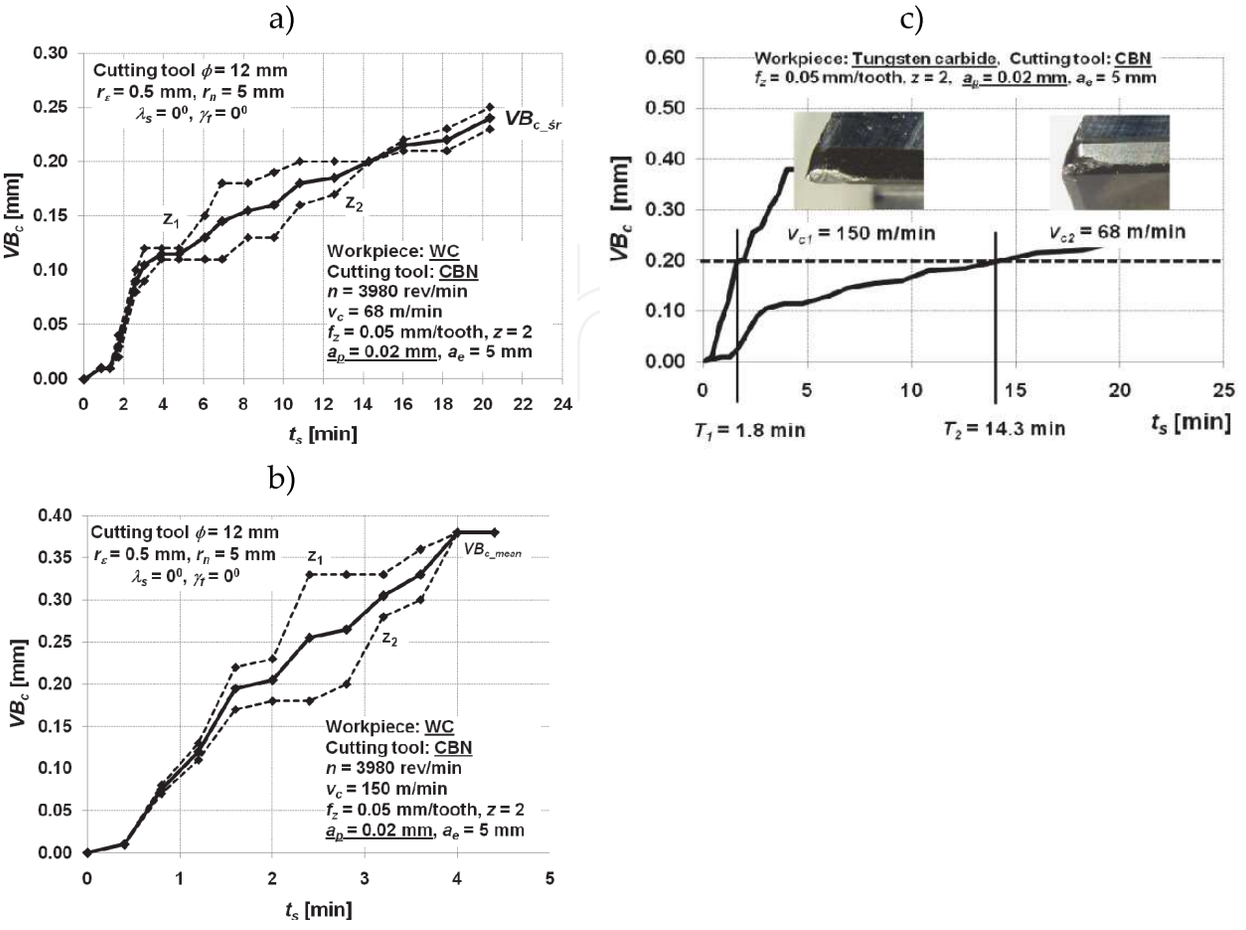

Figure 14. a), b) Tool wear in function of cutting time t_s for two investigated cutting speeds v_c; c) tool wear comparison for exemplary dullness criterion VB_c = 0.2 mm (z_1, z_2 – number of tooth, T_1, T_2 – tool life)

Figure 15 compares the surface texture of tungsten carbide sample manufactured by DLD technology before and after milling.

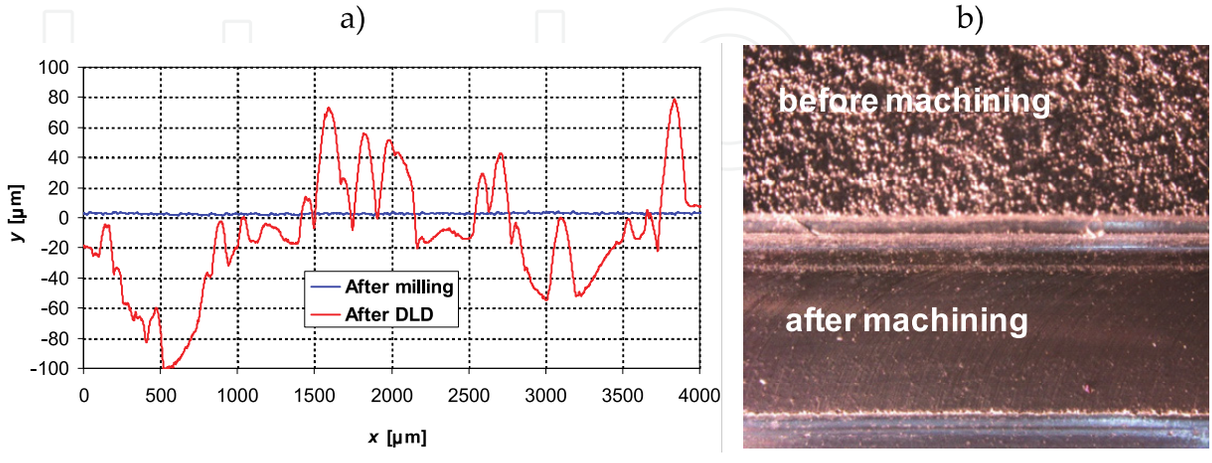

Figure 15. Surface texture of tungsten carbide manufactured by DLD technology, before and after machining: a) 2D surface profile, b) image of surface

It can be seen, that tungsten carbide sample manufactured by DLD technology has an unsatisfactory geometric accuracy and unreasonable surface roughness. Furthermore, from the surface profile and the FFT analysis (Figure 16) it is resulting, that surface texture after DLD process has a random character. The FFT analysis of surface profile consists also of constituent related to the half of the evaluation length (2.4 mm), which means that DLD surface profile is affected by the waviness. Therefore, it needs further finishing process. After milling, machined surface is much smoother and characterized by significantly lower values of surface roughness parameters.

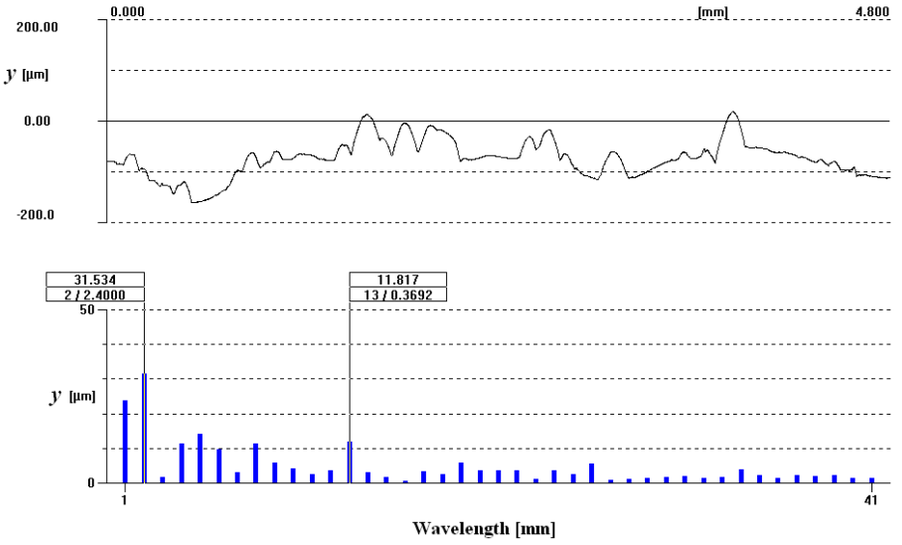

Figure 16. FFT analysis of surface profile after DLD process of tungsten carbide

Figure 17 depicts 3D surface roughness charts and power density spectra (PDS) obtained after milling of tungsten carbide.

It can be seen, that 3D surface topographies after milling (Figure 17) are affected by the cutter's projection into the workpiece. This observation is also confirmed by the power density spectra which represent wavelengths of surface irregularities generated during machining. Surface profiles consist of wavelengths related to the feed per tooth value (f_z = 0.05 mm) which is related to the kinematic-geometric projection of cutter into the workpiece, and feed per revolution value (f = 0.1 mm) which can be induced due to radial run out phenomenon.

Figure 18 depicts examples of profile charts and corresponding to them *Ra* and *Rz* parameters for various feed per tooth f_z values. As it can be seen the fourfold feed per tooth f_z increase did not make any significant qualitative and quantitative surface texture changes. It denotes that feed insignificantly influences surface roughness, what is not in full agreement with the results shown in Figures 17a and 17b. For some instances, characteristic kinematic-geometric projection of cutting edge into the workpiece can be seen, however in a wider surface roughness range, there is no typical relation. Figure 19 depicts surface roughness parameters *Ra* and *Rz* (for v_c = 68 m/min) in function of feed per tooth f_z.

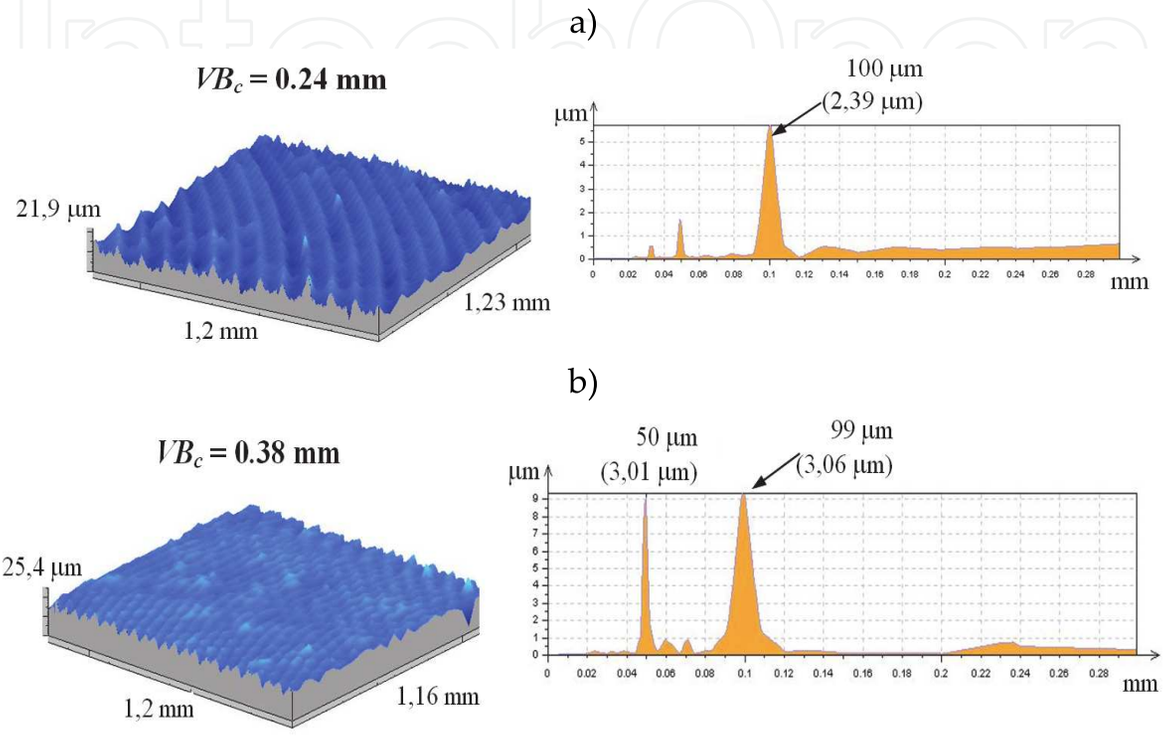

Figure 17. 3D surface roughness chart and corresponding Power Density Function during: a) milling with cutting speed v_c = 68 m/min, b) milling with cutting speed v_c = 150 m/min

From these charts no influence of feed per tooth f_z on surface roughness is seen, despite for f_z = 0.1 mm/tooth. In this case the theoretic value of *Rzt* is comparable to real *Rz* value. It is commonly known that the increase of feed per tooth f_z is accompanied by the increase of surface roughness. Theoretically, the lower feed is fixed, the lower surface roughness is generated. Nevertheless in practice, differences between theoretical and real surface roughness values are increasing with feed decrease. Similar conclusions can be proposed from cumulative *Ra* and *Rz* charts for all a_p and f_z combinations (see Figure 20).

Twofold a_p and fourfold f_z growth caused insignificant *Ra* and *Rz* change. Therefore in the range of conducted research non monotonic increase of surface roughness in function of investigated factors was stated.

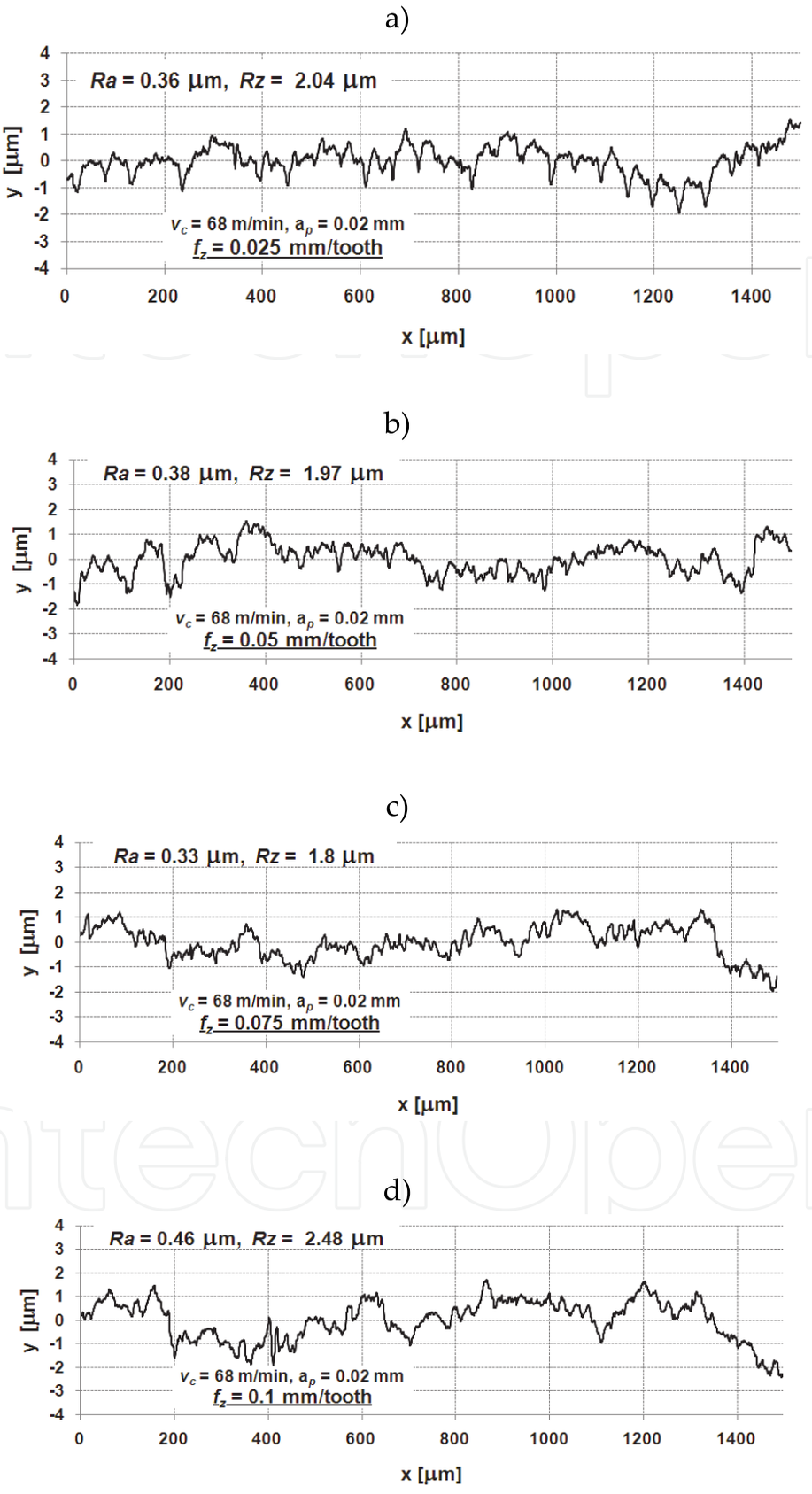

Figure 18. Examples of profile charts for various feed per tooth f_z values: a) f_z = 0.025 mm/tooth, b) f_z = 0.05 mm/tooth, c) f_z = 0.075 mm/tooth, d) f_z = 0.1 mm/tooth

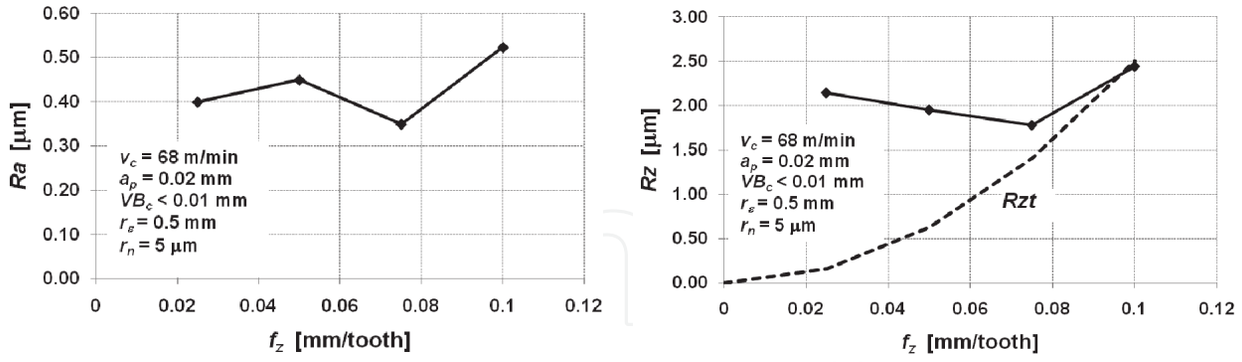

Figure 19. Surface roughness *Ra* and *Rz* in function of feed per tooth f_z

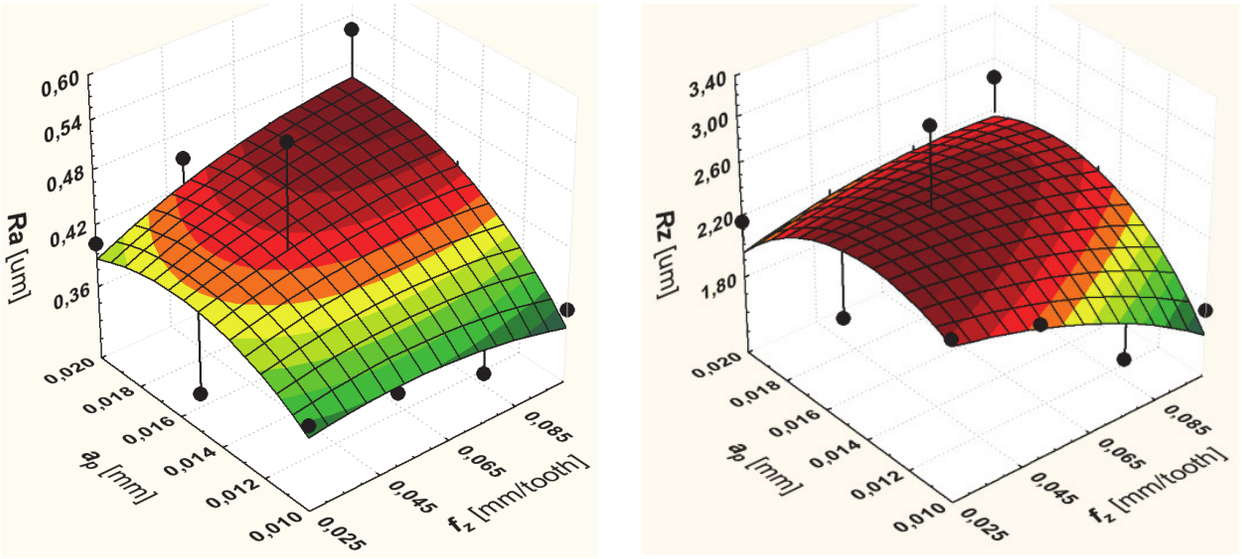

Figure 20. Surface roughness *Ra* and *Rz* in function of feed per tooth f_z and depth of cut a_p

5. Summary and conclusions

The development of modern tool materials such as diamonds (PCD, MCD) and cubic boron nitrides (CBN), as well as ultraprecision and rigid machine tools enables machining of tungsten carbides. These materials have excellent physicochemical properties such as, superior strength, high hardness, high fracture toughness, and high abrasion wear-resistance. On the other hand, these unique properties can cause substantial difficulties during machining process, which can result in low machinability. From the carried out experiments it can be seen, that during machining of tungsten carbides, excessive values of vibrations and intense tool wear growth can occur.

Figure 21 depicts schemes of tungsten carbide products manufacturing processes.

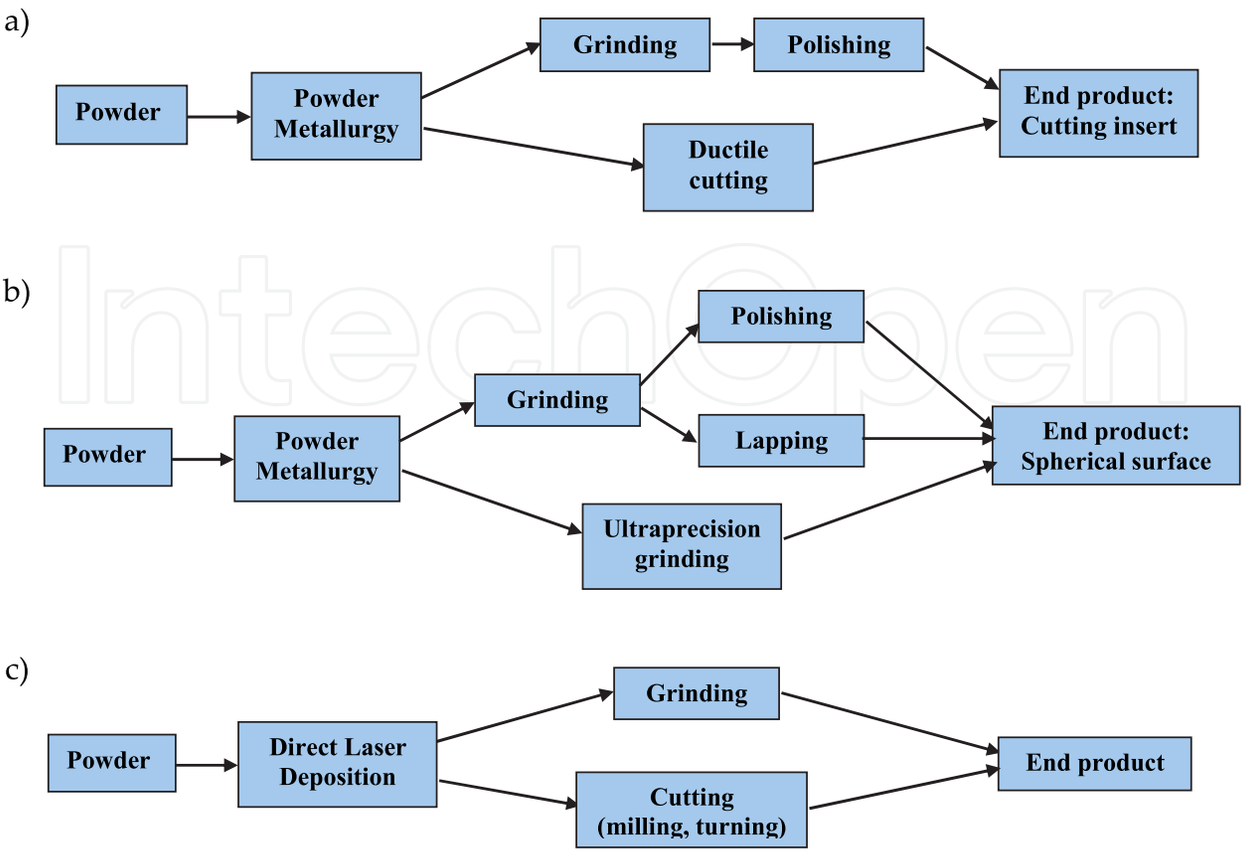

Figure 21. The schemes of manufacturing processes of various products made of tungsten carbide: a) cutting insert, b) spherical surface, c) end product made by DLD technology

The application of ductile cutting to production of cutting inserts (Figure 21a) shortens manufacturing process by the elimination of one partial process (e.g. polishing). However ductile cutting occurs only in the range of extremely low values of depths of cut and feeds. Therefore, this kind of process can be achieved only on very rigid and ultraprecision machine tools, what is substantial limitation of this method. Ultraprecision machine tools can be also applied to grinding of very accurate spherical surfaces. This process also shortens manufacturing process by the elimination of polishing or lapping (Figure 21b). In case of tungsten carbide products obtained by DLD (direct laser deposition) technology (Figure 21c), grinding or cutting (e.g. milling, turning) can be applied as the finishing process. However cutting enables also the shaping of manufactured part, by the possibility of higher cutting conditions application in comparison to grinding. Nevertheless, during cutting of tungsten carbide, intense tool wear growth can occur, and thus this process requires the selection of appropriate cutting conditions.

Deliberations presented in this chapter reveal, that efficient machining process of tungsten carbide parts is feasible, however it requires the knowledge about the physical effects of the process, as well as appropriate selection of machining method and cutting conditions, enabling desired technological effects.

Author details

Paweł Twardowski and Szymon Wojciechowski
Poznan University of Technology, Faculty of Mechanical Engineering, Poznan, Poland

6. References

[1] Schneider G (2002) Cutting Tool Applications. GMRS.
[2] Trent E, Wright P (2000) Metal cutting (4th edition). Butterworth-Heinemann.
[3] Banerjee, R, Collins, P C, Genc A (2003) Fraser, Direct laser deposition of in situ Ti-6Al-4V-TiB composites. Materials Science and Engineering, A358, 343–349.
[4] Fearon E, Watkins K G, (2004) Optimisation of layer height control in direct laser deposition. 23nd International Congress on Applications of Lasers & Electro–Optics (ICALEO 2004), San Francisco, California, Paper No. 1708, Laser Institute of America, Publication No 597, Vol. 97.
[5] http://www.lasercladding.com/
[6] Murphy M, Lee C, Steen W M (1993). Studies in rapid prototyping by laser surface cladding. Proceedings of ICALEO, 882–891.
[7] Taminger K M B, et all (2002). Solid freeform fabrication: An enabling technology for future space missions. Proceedings of International Conference on Metal Powder Deposition for Rapid Manufacturing, San Antonio, 51–60. \
[8] Mazumder J, et al (1999). Direct materials deposition: designed macro– and microstructure. Materials Research Innovations,3, publ. Springer-Verlag, 118–131.
[9] Choi J, Sundaram R (2002). A process planning for 5 – axis laser-aided DMD process. Proceedings of International Conference on Metal Powder Deposition for Rapid Manufacturing, San Antonio, 112–120.
[10] Ling Yin, Spowage A C, Ramesh K, Huang H, Pickering J P, Vancoille E Y J (2004) Influence of microstructure on ultraprecision grinding of cemented carbides. International Journal of Machine Tools & Manufacture 44: 533–543.
[11] Stephenson D J, Vaselovac D, Manley S, Corbett J (2001) Ultra-precision grinding of hard steels. Precision Engineering 25 (4) 336–345.
[12] Yin L, Vancoille E Y J, Lee L C, Huang H, Ramesh K, Liu X D (2004) High-quality grinding of polycrystalline silicon carbide spherical surfaces. Wear 256: 197–207.
[13] Liu K, Li X P (2001) Ductile cutting of tungsten carbide, Journal of Materials Processing Technology, 113: 348-354.
[14] Liu K, Li X P (2001) Modelling of ductile cutting of tungsten carbide, Trans. NAMRI/SME, XXIX 251-258.
[15] Yan J, Zhang Z, Kuriyagawa T (2009) Mechanism for material removal in diamond turning of reaction-bonded silicon carbide, International Journal of Machine Tools & Manufacture, 49: 366-374.
[16] Wojciechowski S, Twardowski P (2010) Cutting forces and vibrations analysis in milling of tungsten carbide with CBN cutters. Proceedings of 4th CIRP International

Conference on High Performance Cutting, 24-26 october, 2010, Nagaragawa Convention Center, Gifu, Japan.
[17] Toenshoff H K, Arendt C, Ben Amor R (2000) Cutting of hardened steel, Annals of the CIRP Vol. 49/2: 546-566.
[18] Liu K, Li X P, Rahman M, Liu X D (2003) CBN tool wear in ductile cutting of tungsten carbide. *Wear*, 255: 1344–1351.
[19] Matsumoto Y, Barash M M, Liu C R, (1987) Cutting mechanisms during machining of hardened steels, Material science and technology, 3, 299 – 305.
[20] Toh C K, (2004) Vibration analysis in high speed rough and finish milling hardened steel, Journal of Sound and Vibration 278: 101–115.
[21] Ning Y, Rahman M, Wong Y S, (2000) Monitoring of chatter in high speed end milling using audio signals method, in: Proceedings of the 33rd International MATADOR Conference, Manchester, England, 421-426.